Using the ARIMA/SARIMA Model for Afghanistans Drought Forecasting Based on Standardized Precipitation Index

Reza Rezaiy and Ani Shabri*

Department of Mathematical Sciences, Faculty of Science, Universiti Teknologi Malaysia
81310 Johor Bahru, Johor, Malaysia
*Corresponding author: ani@utm.my

Abstract Forecasting drought plays a vital role in strategic planning and the management of underground water supply. In this study, we utilized autoregressive integrated moving average (ARIMA) and Seasonal ARIMA (SARIMA) models to predict drought events in Afghanistan, based on the standardized precipitation index (SPI). We used monthly average precipitation data from 1991 to 2015 for model training, while data from 2016 to 2020 were employed for model validation. The results of the statistical analysis, which encompassed evaluating Mean Absolute Error (MAE), Root Mean Squared Error (RMSE), and Mean Absolute Percentage Error (MAPE), indicated that among the SPI 3, SPI 6, SPI 9, SPI 12, and SPI 24, the SARIMA models applied to the SPI 24 demonstrated the most accurate forecasting performance with RMSE (0.1492), MAE (0.1039), and MAPE (22.3732%) compared to SPI 3, SPI 6, SPI 9, and SPI 12. Subsequently, the ARIMA/SARIMA models were employed to forecast drought events for the upcoming year. It's noteworthy that this constitutes the first-ever statistical analysis of the drought index in Afghanistan. Therefore, the outcomes of this study can be applied across diverse sectors, including water resource management and environmental precautions.

Keywords Drought forecasting; Auto-regressive integrated moving average (ARIMA); SARIMA; Time series; SPI; Afghanistan.

Mathematics Subject Classification 62M10, 62M20.

1 Introduction

In recent decades, drought has garnered increased attention as a natural disaster, particularly as climate change and global warming have emerged as some of the most vital issues facing the planet. Drought, recognized as a complex and often underestimated phenomenon, can lead to adverse impacts on the quality of human life. These impacts range from negative effects on agricultural yields and environmental problems to reductions in water supplies and socio-economic consequences [1]. Although there is no universal consensus on the definition of drought, it is generally characterized as a lack of soil moisture over sustained periods, resulting in decreased water supplies and groundwater

levels dropping below the normal average for a given region. Consequently, this leads to an increased demand for water. As a result, various definitions of drought have been proposed, encompassing meteorological, hydrological, agricultural, and socio-economic perspectives. [2], [3], [4], [5].

Drought is a phenomenon that occurs gradually and may persists for short periods (months or seasons) or extend for years. However, drought is an inevitable event and can have negative effects on society. Forecasting the occurrence of drought in advance is one of the most reasonable measures that can help mitigate its effects. Drought possesses distinct characteristics compared to other natural hazards. Firstly, drought does not have an early onset and is recognized as a creeping threat. Because the start of a drought period cannot be determined in advance, having an early drought alert system and predicting its signals becomes crucial for policymakers and precise risk management [6]. Secondly, since the fundamental factors of drought are unpredictable, it is considered a stochastic process that can impact all aspects of environmental quality and human lives [7]. By detecting drought early, the adverse impacts of drought can be mitigated. Drought forecasting plays a pivotal role in water resources management and planning. Consequently, mitigating the effects of drought presents a challenging approach in risk management and policy-making. Several approaches address the shortfall in rainfall and aim to enhance the efficiency of drought monitoring [8].

There are several indices available for assessing meteorological drought and identifying its occurrences, including the Effective Drought Index (EDI), Reconnaissance Drought Index (RDI), Palmer Drought Severity Index (PDSI), Standard Precipitation Evaporation Index (SPEI), and SPI. Among these, SPI stands out as one of the most widely used indices for evaluating the severity of drought, as indicated by the World Meteorological Organization (WMO) report [9]. Research indicates several benefits associated with using SPI to assess drought intensity. Firstly, the calculation of SPI is less complex, and it serves as a standardized index that can be applied across various regions. Secondly, SPI is a flexible index that can describe drought under different conditions, allowing for variations in timescales. Another advantage of SPI is that its calculation relies solely on precipitation data, making it highly efficient in areas where other parameters such as temperature, evaporation, and soil moisture are unavailable [10], [11]. Therefore, in the current study, SPI was chosen as the meteorological drought index.

Drought is a natural phenomenon that occurs gradually and often goes unnoticed until it has already happened. Consequently, forecasting drought holds a significant role within early warning systems and in mitigating potential adverse impacts. Therefore, various methodologies are employed in drought forecasting, encompassing stochastic models [1], [12], [13], regression analysis [14], [15], artificial neural networks [16], [17], [18], probabilistic models [19], and dynamic modeling [20]. One of the most popular and widely used approaches in drought studies is time series modeling. An exemplar of these models are the ARIMA and SARIMA models.

Despite certain limitations in handling non-stationary and nonlinear models, the ARIMA/SARIMA model is frequently employed in drought prediction due to its numerous advantages. Initially, the ARIMA/SARIMA model possesses a remarkable ability to handle linear data sets, rendering it suitable for modeling stream flow and precipitation processes [21]. Additionally, the ARIMA/SARIMA model offers a structured search process for identifying an appropriate model at each stage of the process, including identification, estimation, and diagnostic checking [22]. Moreover, this model demonstrates a strong capability in recognizing serial autocorrelation among observations, a trait commonly present in time-oriented datasets, and accurately characterizes this feature [1]. Further benefits include its ability to model non-stationary processes, its straightforward computational procedures, low data input requirements [13], and a

parsimonious number of parameters needed to describe the time series models [23]. Furthermore, several studies have indicated that the ARIMA/SARIMA model holds a significant advantage over other statistical approaches, such as exponential smoothing and neural networks, in hydrological time series analysis [1]. Given these advantages, the ARIMA model has gained widespread use and is regarded as an essential method for predicting drought events.

Afghanistan, being an agricultural country reliant on winter rainfall and snow, is currently grappling with a severe drought exacerbated by climate change. Reports from the Food and Agriculture Organization of the United Nations (FAO) indicate that significant portions of the country have witnessed a substantial decline in precipitation, with reductions of up to 70 percent during the traditionally wet months, commencing from the 2018 planting year. This extreme dryness and shortfall in rainfall have adversely affected agricultural crops and the economy of the nation [24]. While international organizations have published reports on drought in Afghanistan, there is a notable absence of scientific studies addressing drought forecasting specifically for the region.

Consequently, the primary objective of this study is to establish a suitable forecasting model based on the SPI for predicting drought in Afghanistan. Such a model holds the potential to assist the Afghan government and officials in devising appropriate measures and managing critical drought periods to mitigate the adverse impacts of this natural phenomenon. A linear stochastic model is anticipated to be advantageous for predicting the SPI series, given that SPI calculations rely on averaging precipitation series.

This research holds significance for the following reasons: a) The study area has endured four decades of war, resulting in infrastructural damage, and being an underdeveloped nation, there is a dearth of previous drought analyses; b) A large proportion of Afghanistan's population is economically dependent on agriculture, particularly the impoverished populace. Consequently, the prediction of drought events is deemed essential for both policy makers and the general populace.

2 Study Area and Data

Afghanistan, a mountainous country situated at the crossroads of central and south Asia, is characterized by its diverse landscape. Its geographical coordinates are latitude 33.93911 and longitude 67.709953 Sharing borders with Pakistan to the east and south, Iran to the west, Turkmenistan, Uzbekistan, and Tajikistan to the north, and China to the northeast, Afghanistan occupies a total area of 652,000 square kilometers (Figure 1). The country possesses a continental climate, exhibiting distinct variations. The climate ranges from dry in the south and southeast to semi-arid in the north and other regions. Much of the Afghan population resides amidst fertile valleys and mountains, with a significant proportion reliant on subsistence agriculture and farming. Notably, temperature fluctuations between summer and winter are quite pronounced. While winter precipitation is primarily in the form of snow, summer temperatures soar while precipitation becomes minimal. The high mountain ranges of Hindu Kush and Pamir, reaching altitudes above 5000 meters, are predominantly characterized by permanent snow and glaciers. These areas experience a humid climate. In Afghanistan, water resources heavily rely on the efficient distribution of precipitation. Consequently, the arid to semi-arid nature of this region makes it unsuitable for irrigation without the presence of irrigation reservoirs.

Afghanistan has been grappling with a severe to below-normal drought situation, which has significantly affected the accessibility and availability of clean drinking water. According to [25],
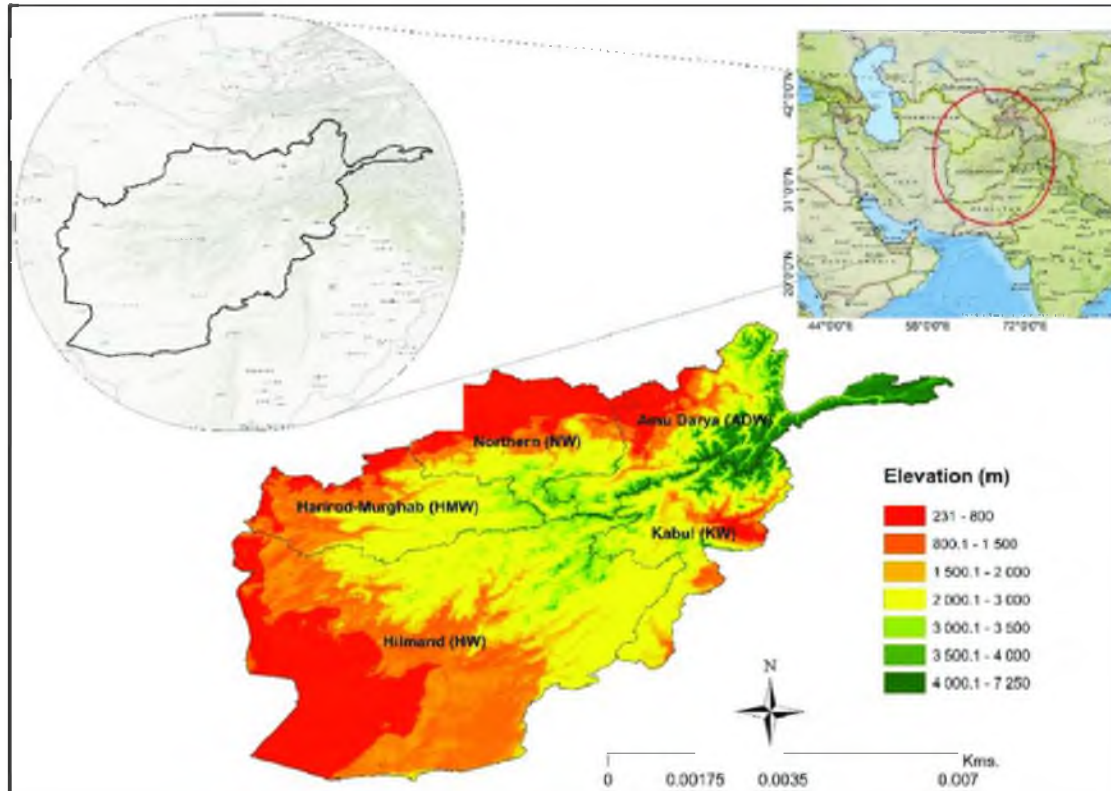
Figure 1. A location map of the study area, Afghanistan.

approximately 79 percent of homeowners have reported inadequate access to water for fundamental necessities such as drinking, cooking, bathing, and maintaining hygiene. Consequently, by anticipating drought conditions, policymakers and water supply managers can proactively mitigate its potentially catastrophic effects through prudent precautions. In this study, the monthly average precipitation data spanning from 1991 to 2020 was sourced from the World Bank Climate Change Knowledge Portal (https://climateknowledgeportal.worldbank.org) to facilitate an analysis of drought forecasting in Afghanistan.

3 Methodology

3.1 Standardized Precipitation Index

As previously mentioned, there exist several drought indices for identifying drought conditions. One of the most commonly utilized indices in the realm of drought forecasting is the SPI. Conversely, other drought indices are applicable only in specific regions and necessitate extensive data and intricate procedures for implementation. Despite the availability of numerous indices, the WMO has endeavored to establish a unified standard index that can serve as a baseline for all regions and countries [2]. In 2009, the SPI was proposed as a prominent drought index to be universally calculated and employed by meteorological and hydrological agencies [26].

Originally formulated by [27], the SPI employs historical precipitation data in spatial analysis,

encompassing both positive and negative values. Positive values signify surplus while negative values indicate deficiency events. The SPI possesses two key advantages: it can be calculated even in the presence of missing data, and its applicability spans distinct time intervals, accommodating both short and long durations [2]. As outlined in [17], the SPI can be derived by fitting a Gamma distribution to monthly precipitation aggregated series over varying time frames (3, 6, 9, 12, and 24 months). For instance, SPI 3 focuses on three-month moisture fluctuations, whereas SPI 12 offers a year-long perspective by accounting for precipitation variations. With SPI 3 capturing recent changes and SPI 12 reflecting longer-term patterns, both indices are employed to analyze and monitor drought and wetness conditions. Gamma distribution is used to fit lengthy periods of historical rainfall records because it closely matches the sequence of rainfall episodes. The probability density function (PDF) derived from the gamma distribution is shown in equation (1).

$$f(x; \alpha; \beta) = \frac{1}{\beta^\alpha \Gamma(\alpha)} x^{\alpha-1} e^{-\frac{x}{\beta}} \qquad for \ x, \alpha, \beta > 0 \tag{1}$$

where $\beta, \alpha, x, \Gamma(x)$ representing the scale, shape variables, quantity of precipitation, and gamma function respectively. Equation (2) provides the best estimates for α and β [28].

$$\hat{\alpha} = \frac{1}{4A}\left(1 + \sqrt{1 + \frac{4A}{3}}\right), \qquad \hat{\beta} = \frac{\bar{x}}{\alpha} \tag{2}$$

where the precipitation average and the total number of observations are represented by the letters x and n, respectively.

$$A = ln(\bar{x}) - \frac{\sum ln(x)}{n} \tag{3}$$

$$F(x; \alpha, \beta) = \int_0^x f(x, \alpha, \beta) dx = \frac{1}{\beta^\alpha \Gamma(\alpha)} x^{\alpha-1} e^{-\frac{x}{\beta}} dx \tag{4}$$

The variables required to calculate the cumulative probability for non-zero precipitations are shown in Equation (5).

$$F(x; \alpha, \beta) = \frac{1}{\Gamma(\alpha)} \int_0^x t^{\alpha-1} e^{-t} dt \tag{5}$$

where $t = \frac{x}{\beta}$. For $x = 0$, the gamma function is uncertain, the precipitation time series data may include zero precipitation, the cumulative probability of zero and non-zero precipitation is calculated, and equation (6) is used to determine H(x).

$$H(x) = q + (1-q)F(x; \alpha, \beta) \tag{6}$$

where q, denotes the probability of no precipitation and the number of zeros (which occur in a rainfall time series). Once the cumulative probability is changed to a standardized normal distribution [1], as demonstrated by Equations (7) and (8), the SPI mean and variance would equal zero and one, respectively.

$$SPI = -\left(k - \frac{c_0 + c_1 k + c_2 k^2}{1 + d_1 k + d_2 k^2 + d_3 k^3}\right), \qquad when \ k = \sqrt{ln\left(\frac{1}{(H(x))^2}\right)} \tag{7}$$

for $0 < H(x) \leq 0.5$

$$SPI = + \left(k - \frac{c_0 + c_1 k + c_2 k^2}{1 + d_1 k + d_2 k^2 + d_3 k^3}\right), \qquad when \quad k = \sqrt{ln\left(\frac{1}{(1 - H(x))^2}\right)} \tag{8}$$

for $0 < H(x) \leq 1$.

In equations (7), and (8) $c_0 = 2.515517$, $c_1 = 0.802853$, $c_2 = 0.010328$ $d_1 = 1.432788$, $d_2 = 0.189269$, and $d_3 = 0.001308$. Table 1 presents the SPI classifications.

Table 1: Weather classification based on SPI [1], [29]

SPI value	Category
SPI > 2	Extremely wet
1.5 < SPI ≤ 2	Very wet
1 < SPI ≤ 1.5	Moderately wet
-1 < SPI ≤ 1	Nearly Normal
-1.5 < SPI ≤ -1	Moderate drought
-2 ≤ SPI ≤ -1.5	Severe drought
SPI < -2	Extreme drought

3.2 Time Series Model

Time series models, also referred to as linear stochastic models, have garnered increased attention in the domain of meteorological and hydrological drought over the past few decades [12], [13]. Among the various time series models, two particularly prominent ones used extensively in drought forecasting are the ARIMA and the SARIMA, which will be elucidated as follows.

3.2.1 ARIMA Model

One of the most common and useful method in time series analysis is autoregressive moving average (ARMA) model which is consisted from combination of two effective simpler models including autoregressive (AR) and moving average (MA). ARMA model which only can be applied in stationary records expresses the current value of time series as linear regression of p previous values and weighted sum of values deviation plus white noise. Other class of time series which is applicable in non-stationary records can be obtained by allowing referencing data series which is called autoregressive integrated moving average (ARIMA) model. This class of time series model initially suggested by [30], the general non-seasonal ARIMA contains AR to order p, MA to order q, and dth operators for differentiating the original time series z_t. This model can be illustrated as $ARIMA(p, d, q)$ and could be written as follows:

$$\phi(B)\nabla^d z_t = \theta(B)\varepsilon_t \tag{9}$$

where $\phi(B)$ and $\theta(B)$ are polynomials of order p and q respectively, while ε_t is a time-independent uncorrelated variable having mean μ and variance σ^2 and ∇^d is non-seasonal differencing. The operators $\phi(B)$ and $\theta(B)$ will be described as follows:

$$\phi(B) = (1 - \phi_1 B - \phi_2 B^2 - \dots - \phi_p B^p) \tag{10}$$

$$\theta(B) = (1 - \theta_1 B - \theta_2 B^2 - \dots - \theta_q B^q) \tag{11}$$

3.2.2 SARIMA Model

Many time series in the field of hydrology have cyclic properties. To address a non-stationary time series with seasonal features [31] expanded the ARIMA model and introduced the seasonal autoregressive integrated moving average (SARIMA) model. Generally, the SARIMA model known as $SARIMA(p, d, q)(P, D, Q)_S$ which the (p, d, q) illustrating the non-seasonal part of the original series while, the seasonal part of the series will be described by $(P, D, Q)_S$ that can be written as bellow:

$$\phi_p(B)\Phi_P(B^s)\nabla_d\nabla_s^D z_t = \theta_q(B)\Theta_Q(B^s)\varepsilon_t \tag{12}$$

Based on the equation (12) p is the order of nonseasonal AR model, q is the order of nonseasonal MA model, d is the number of regular differencing, P the order of seasonal autoregression, D the number of seasonal differencing, Q the order of seasonal MA, and eventually s is the length of season. B shows the backward operators, Φ is seasonal autoregressive, ϕ indicates non-seasonal autoregressive, ∇^D is seasonal differencing, ∇_d is non-seasonal differencing, Θ is non-seasonal differencing, and θ represents a non-seasonal moving average.

3.3 Development of the ARIMA/SARIMA model

Development and selection of a suitable model for the specific time-oriented records is a crucial step in the implementation of the ARIMA/SARIMA model. Figure 2 provides an overview of the model development process. The extension of the ARIMA/SARIMA model, comprising three stages—model identification, parameter estimation, and diagnostic checking—can be accomplished through an iterative operation, as elaborated in the subsequent sections [1], [32], [33], [34].

3.3.1 Model Identification

The objective of identification is to select a subclass of the ARIMA/SARIMA family of models that effectively captures the characteristics of the time series. As outlined in [30], the identification stage involves a preliminary process of establishing an initial model structure that reasonably aligns with the collected observational data. The general form of the model is determined through two steps: (1) Analyzing the autocorrelation function (ACF) and partial autocorrelation function (PACF) of the transformed data to identify the temporal correlation structure [1]. (2) If necessary, applying suitable differencing to the series to achieve stationarity. This information is then used to define the overall shape of the model to be fitted.

The ACF is a practical statistical tool used to determine if early values in a series are related to subsequent values. The ACF ranges continuously between -1 and 1, with a value of 1 at lag number 0. The ACF primarily examines autocorrelation between neighboring data points, such as between observations 1 and 2, 2 and 3, 3 and 4, and so on. Typically, the autocorrelation test is conducted at delays ranging from one to $n/4$, where n represents the total number of observations. For this investigation, a total of 360 observations were collected. Research has shown that estimates with longer delays are statistically unreliable [13]. The PACF mitigates the influence of shorter lag autocorrelation, thereby reducing correlation estimates at longer delays. PACF quantifies the portion
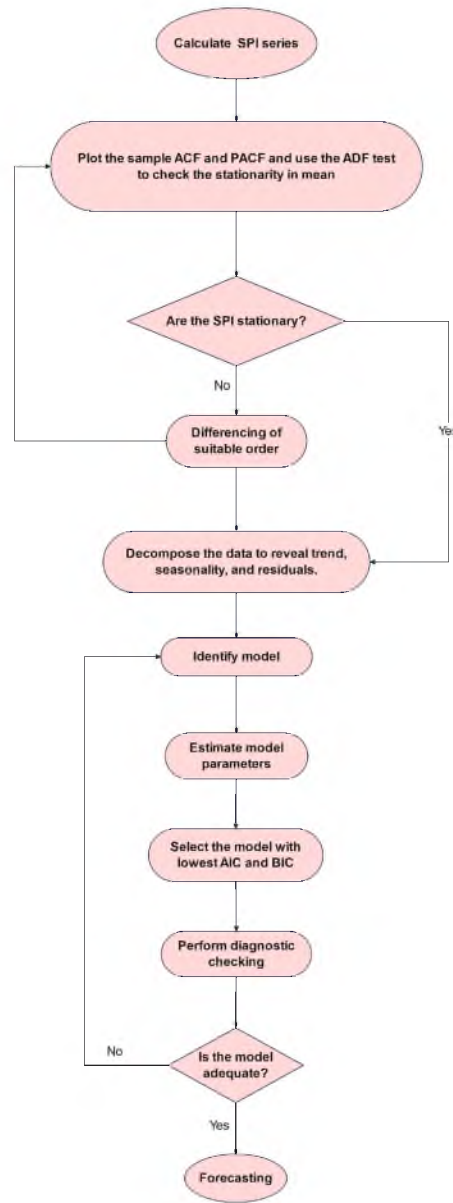
Figure 2. ARIMA/SARIMA Framework.

of correlation between a variable and its own lag that is not explained by correlations at lower-order delays.

The final model's accuracy will be assessed using goodness-of-fit criteria, specifically the Akaike information criterion (AIC) and the Schwarz Bayesian criterion (BIC) [35], [36]. The mathematical formulation of these criteria is described below:

$$AIC = -2log(L) + 2k \tag{13}$$

$$BIC = -2log(L) + kln(L) \tag{14}$$

where k is illustrating the number of parameters in the model $(p + q + P + Q)$, L is the likelihood function of the ARIMA/SARIMA model, and n is the number of data in the model. The model with the minimum of AIC and BIC will be recommended as the best model.

3.3.2   Parameter Estimation

Once the appropriate model has been identified based on the AIC and BIC criteria, the next step involves estimating the model's parameters. Various methods are available for estimating unknown parameters, including the methods of moments, maximum likelihood, and least squares. In this particular study, following the approach outlined in [30], the unknown parameters of the model will be estimated using the maximum likelihood method—a statistical technique employed for parameter estimation within a model. An appealing aspect of the maximum likelihood method is its versatility; unlike other methods, such as the Cochrane-Orcutt method, it can be utilized in scenarios where the autocorrelation structure of the errors is more intricate than simple first-order autoregressive structures [37].

3.3.3   Diagnostic Checking

Upon selecting the appropriate model and calculating the unknown parameters, it becomes necessary to assess the adequacy of the model and propose potential enhancements if required. The objective of this stage is to ensure that the model's residuals exhibit characteristics of independence, adhere to a normal distribution, and demonstrate homoscedasticity. These conditions are essential to establish the suitability of the current time series model. To achieve this, several tests and residual plots are recommended. The white noise process serves as an indicator of the model's validity: if the residuals conform to a white noise process, characterized by being uncorrelated and distributed around zero, then the model can be deemed suitable.

One approach to assessing the independence of the series is by examining the residuals of ACF and PACF. If the ACF and PACF residuals fall within the confidence interval, it can be inferred that there is no significant correlation among the residuals. Alternatively, the Ljung-Box-Pierce (LBQ) test can serve as an alternative method to achieve this objective. The LBQ test is a statistical assessment designed to determine the independence of residuals. The test statistic is formulated as follows:

$$Q = n(n + 2) \sum_{k=1}^{m} \frac{r_k^2}{n - k} \tag{15}$$

where the r_k is indicating the sample autocorrelation at lag k, n the number of data, and m is the number of autocorrelation lags. The null hypothesis of the LBQ statistic is the residuals are independent. Q

is approximately distributed as chi-square with $m - p - q$ degrees of freedom. The obtained value of Q if will be too large, so it is indicating that the model is inadequate. Therefore, the hypothesis of the model adequacy will be rejected if Q exceeds an approximate small upper tail point of the chi-square distribution with $m - p - q$ degrees of freedom [38]. To assess the normality of residuals, histograms and normal probability plots can be employed. To examine homoscedasticity, a scatter plot of residuals against predicted values is useful. If the scatter plot lacks discernible patterns, it indicates that the assumption of constant error variance across the data is satisfied.
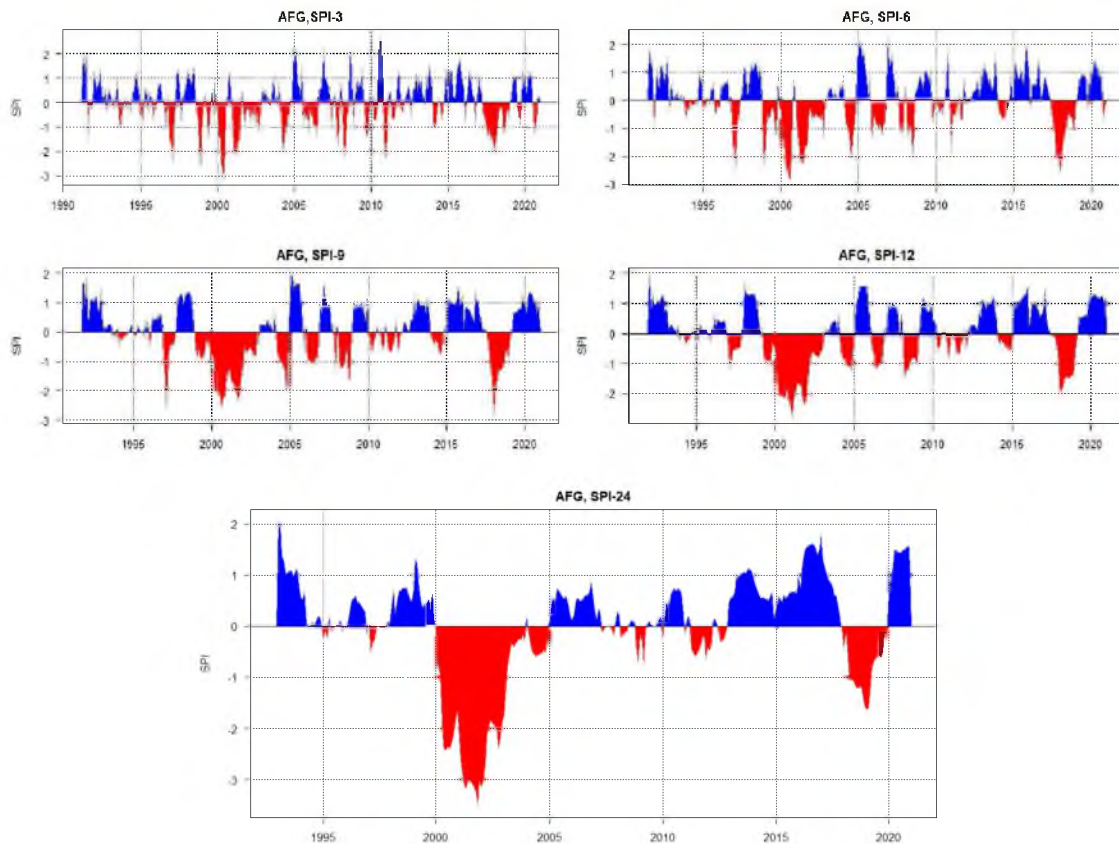

Figure 3. SPI time series based on the average precipitation over the Afghanistan (the case study).

3.3.4   Forecasting Evaluation Methods

In this study, we utilized three distinct statistical criteria to gauge the forecasting performance and the reliability of the proposed prototype, ensuring the model's accuracy. These criteria encompass: Root Mean Square Error (RMSE): This metric illustrates the standard deviation of the forecasted quantities generated by the model. It gauges the extent of deviations between predicted and actual data ; Mean Absolute Error (MAE): By calculating the average difference between observed data and projected results, MAE measures the precision of the model's predictions; Mean Absolute Percentage Error (MAPE): This criterion evaluates the precision of forecasted values relative to the actual quantities. It quantifies discrepancies in terms of percentages. By employing these three criteria, a comprehensive

evaluation of the model's forecasting performance and its dependability is established.

$$RMSE = \sqrt{\frac{1}{n}\sum_{i=1}^{n}(Y_i - \hat{Y}_i)^2} \tag{16}$$

$$MAE = \frac{1}{n}\sum_{i=1}^{n}|Y_i - \hat{Y}_i| \tag{17}$$

$$MAPE = \frac{1}{n}\sum_{i=1}^{n}|\frac{Y_i - \hat{Y}_i}{Y_i}| \times 100 \tag{18}$$

In equations (16) to (18) n representing the number of data, Y_i indicates the observed data, and $\hat{Y}_i$ is illustrating the predicted data. Based on these criteria, a better model performance will be gained with smaller RMSE and MAE, and MAPE values.

4 Results and Discussion

In the present study, we utilized the ARIMA model to predict drought events in Afghanistan, using the SPI as our basis. The dataset was partitioned into two discrete periods: a training phase encompassing the years 1991 to 2015, and a subsequent validation phase spanning from 2016 to 2020. The progression of model development involved three key stages: identifying the model, estimating unknown parameters, and conducting diagnostic checks. Throughout this study, we employed the R software for both the development of the model and the prediction of future drought incidents.

4.1 Model Identification

Multiple time scales of SPI, including SPI 3, SPI 6, SPI 9, SPI 12, and SPI 24 (depicted in Figure 3), were computed based on historical records. Examination of the 3-month SPI time series unveiled instances of extreme drought (SPI < -2) occurring in several years. A analysis of the relative frequency illustrated that Afghanistan faced extreme drought in specific months, such as February 1997, December 1998, April and May 2000, March and April 2001, April 2008, December 2010, January 2011, and January 2018. Evaluating the 6-month SPI demonstrated that extreme droughts were predominantly observed during the summer, with the year 2000 experiencing continuous extreme drought from May to September. Investigation of the 9-month SPI highlighted relatively frequent droughts during the periods of 2000-2001, late 2004, and early 1997 and 2018. Further analysis of the SPI 12 and SPI 24 indicated that Afghanistan encountered episodes of extreme drought in the spring and summer of 2000, 2001, and 2002. Notably, the annual precipitation for the years 2000 to 2002 marked the lowest levels within the 30-year analysis period. The drought witnessed during 2000 to 2002 stands out as the most severe drought ever recorded in Afghanistan's history.

The objective of model identification is to determine a suitable subclass of the ARIMA model that fits the time series data accurately. Initially, the stationarity of the records is examined. To achieve this, the Augmented Dickey-Fuller (ADF) test was employed. The outcomes affirmed that, except for SPI 24, the remaining four SPI values exhibited stationarity. Consequently, differencing was applied to SPI 24. Upon implementing the first-order differencing, all SPI values fulfilled the conditions
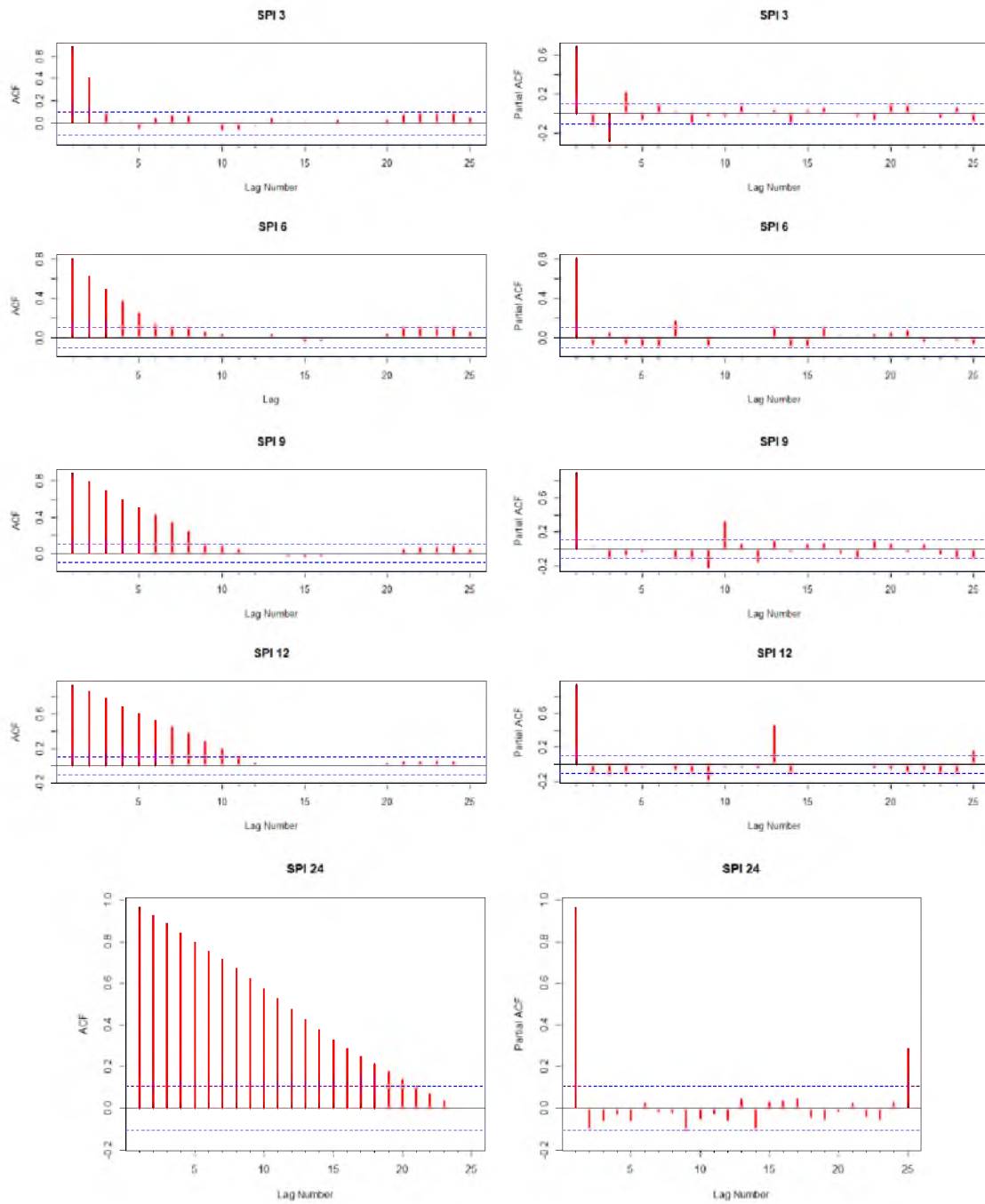
Figure 4. ACF and PACF plots used for the selection of candidate models for SPI 3, 6, 9, 12, and 24.

Table 2: The AIC and BIC criterion parameters of each SPI series for selected candidate ARIMA models.

SPI series	Model	AIC	BIC
SPI 3	ARIMA(2,0,2)	636.79	658.97
	ARIMA(3,0,1)	636.53	658.71
	ARIMA(4,0,0)	637.67	659.85
	$ARIMA(1,0,0)(1,0,0)_3$	640.31	655.10
	$ARIMA(2,0,2)(1,0,0)_3$	637.66	663.54
	$ARIMA(3,0,1)(2,0,0)_3$	639.45	669.03
SPI 6	$ARIMA(1,0,0)(1,0,0)_6$	528.89	543.64
	$ARIMA(2,0,2)(0,0,1)_6$	526.36	552.17
	$ARIMA(2,0,2)(2,0,0)_6$	528.05	557.55
	$ARIMA(2,0,1)(1,0,0)_6$	528.03	550.16
	$ARIMA(2,0,1)(2,0,0)_6$	526.56	552.37
	$ARIMA(2,0,1)(1,0,1)_6$	526.69	552.5
	$ARIMA(1,0,0)(0,0,1)_6$	525.29	540.04
SPI 9	$ARIMA(2,0,2)(1,0,1)_9$	315.85	345.26
	$ARIMA(1,0,0)(1,0,0)_9$	323.44	338.15
	$ARIMA(1,0,2)(2,0,0)_9$	320.32	346.06
	$ARIMA(2,0,1)(2,0,1)_9$	315.01	344.43
	$ARIMA(1,0,1)(1,0,1)_9$	313.83	335.89
	$ARIMA(1,0,0)(2,0,0)_9$	318.89	337.27
	$ARIMA(1,0,0)(0,0,1)_9$	310.35	325.06
SPI 12	$ARIMA(2,0,2)(0,0,1)_{12}$	79.41	105.08
	$ARIMA(2,0,2)(2,0,2)_{12}$	73.76	110.43
	$ARIMA(1,0,2)(1,0,2)_{12}$	69.93	99.27
	$ARIMA(2,0,1)(1,0,2)_{12}$	72.38	101.72
	$ARIMA(1,0,1)(1,0,2)_{12}$	70.12	95.79
	$ARIMA(3,0,1)(1,0,2)_{12}$	71.87	104.86
	$ARIMA(1,0,0)(1,0,1)_{12}$	73.14	91.48
SPI 24	$ARIMA(2,1,2)(1,0,1)_{24}$	-86.69	-61.34
	$ARIMA(0,1,1)(0,0,1)_{24}$	-92.78	-81.92
	$ARIMA(0,1,0)(0,0,1)_{24}$	-90.57	-83.32
	$ARIMA(0,1,0)(2,0,2)_{24}$	-86.83	-68.73
	$ARIMA(0,1,0)(1,0,2)_{24}$	-88.64	-74.16
	$ARIMA(1,1,0)(1,0,1)_{24}$	-92.24	-77.76
	$ARIMA(1,1,0)(0,0,1)_{24}$	-93.08	-82.22
	$ARIMA(0,1,1)(1,0,2)_{24}$	-89.72	-71.62
	$ARIMA(0,1,0)(2,0,1)_{24}$	-88.69	-74.21
	$ARIMA(3,1,2)(1,0,1)_{24}$	-96.26	-67.3

necessary for model development. Figure 4 illustrates the ACF and PACF plots for the original time series of SPI 3, SPI 6, SPI 9, SPI 12, and SPI 24. Various ARIMA models were fitted to the SPI time series data. The selection of the optimal model is based on the AIC and BIC criteria. The model with the lowest AIC and BIC values will be chosen as the most suitable option.

Several models have been fitted to the multiple SPI time scales. According to the AIC and BIC criteria in table 2, best models for SPI 3, SPI 6, SPI 9, SPI 12, and SPI 24 are $ARIMA(3,0,1)$, $SARIMA(1,0,0)(0,0,1)_6$, $SARIMA(1,0,0)(0,0,1)_9$, $SARIMA(1,0,0)(1,0,1)_{12}$, and $SARIMA$ $(1,1,0)(0,0,1)_{24}$ respectively.

4.2 Parameter Estimation

Following the identification of the optimal ARIMA model for each SPI time scale, the model parameters were estimated. The results, as displayed in Table 3, include the model parameters, standard error, t-statistic, and p-value. It is evident that the standard error is relatively low in comparison to the model parameter values. Moreover, the majority of p-values in the model are statistically significant, indicating that these parameters can be retained in the models [39].

Table 3: Statistical analysis of the model parameters for SPI time scales

SPI Series Model Parameters		Variables in the Model			
		Value of Parameter	Standard Error	t-Statistic	p-Value
SPI 3	constant	0.0255	0.0939	0.2724	0.7852
	ϕ_1	0.2515	0.0965	2.6061	0.0091
	ϕ_2	0.4596	0.0700	6.5635	0.0000
	ϕ_3	-0.3630	0.0550	-6.5944	0.0000
	θ_1	0.5365	0.0932	5.7586	0.0000
SPI 6	constant	0.0235	0.1483	0.1587	0.8739
	ϕ_1	0.8426	0.0332	25.3437	0.0000
	Θ_1	-0.3041	0.0616	-4.9392	0.0000
SPI 9	constant	0.0363	0.2142	0.1693	0.8655
	ϕ_1	0.9502	0.0203	46.7733	0.0000
	Θ_1	-0.5447	0.0564	-9.6640	0.0000
SPI 12	constant	0.1812	0.3762	0.4816	0.6300
	ϕ_1	0.9866	0.0099	99.4667	0.0000
	Φ_1	-0.2052	0.0863	-2.3776	0.0174
	Θ_1	-0.5775	0.0767	-7.5260	0.0000
SPI 24	ϕ_1	0.1275	0.0598	2.1337	0.0329
	Θ_1	-0.6460	0.0649	-9.9589	0.0000

4.3 Diagnostic Checking

Upon completing parameter estimation, it is essential to conduct diagnostic checks on the model. This entails scrutinizing the residuals of the model and ensuring adherence to the white noise condition process. The residuals must fulfill the following three statistical criteria: (1) the residuals should

Table 4: Ljung–Box–Pierce (LBQ) statistics for SPI Series

SPI Series	LBQ Test				
	SPI 3	SPI 6	SPI 9	SPI 12	SPI 24
x-Squared	0.0788	0.1015	0.5918	1.3552	0.0286
p-Value	0.7790	0.7501	0.4417	0.2444	0.8657

exhibit independence from one another; (2) the probability distribution of residuals must conform to a normal distribution; (3) the residuals should demonstrate constant variance, satisfying the condition of homoscedasticity.

For examining the residuals of the model we have utilized two common approaches. First, the residuals were checked by the correlogram. Figures 5 illustrates the Residual ACF (RACF) and Residual PACF (RPACF) values of each SPI time scales. According to the results from the RACF and RPACF, it can easily found that the residuals does not show the significant correlation with each other and most of the residuals values located in the confidence interval limitations. For the second method, the LBQ test was applied to determine whether the residuals are independent or not. The results from this test in Table 4 indicates that residuals of each SPI values in different time scales were not correlated and satisfy the white noise properties process.

To check the normalization assumption of the residuals the histogram and normal probability of residuals were used. Figure 6 shows histogram and normal probability of residuals in every SPI values. The histograms of the residuals are shown in this figure, which does not reveal a serious deviation from normality and therefore meet the normality assumption [38]. The normal probability plot of the residuals illustrates which residuals of each models lay on a diagonal line which confirms the normality of the assumptions approximately [40], [41]. Although in SPI 12 and SPI 24, the normal probability plot (QQ plot) appears to show the data deviating from a normal distribution, it's important to note that the adequacy of the model is supported by the results of the Ljung-Box test, as well as the examination of the ACF and PACF.

Table 5: Performance measures for the selected model for the observed data and predicted values

SPI Series	Model	Performance Measures		
		RMSE	MAE	MAPE
SPI 3	$ARIMA(3,0,1)$	0.5559	0.4368	103.2368
SPI 6	$ARIMA(1,0,0)(0,0,1)_6$	0.4787	0.3494	125.8515
SPI 9	$ARIMA(1,0,0)(0,0,1)_9$	0.3598	0.2659	74.3730
SPI 12	$ARIMA(1,0,0)(1,0,1)_{12}$	0.2255	0.1578	128.8911
SPI 24	$ARIMA(1,1,0)(0,0,1)_{24}$	0.1492	0.1039	22.3732

To assess the homoscedasticity of the residuals and determine the consistency of the fitted models in predicting variable values, scatterplots of the residuals against the predicted values were generated. Figure 7 depicts scatter plots of residuals for each SPI series plotted against their corresponding fitted values. The outcomes of this analysis revealed that all of these scatter plots do not exhibit any discernible pattern, indicating that the residuals are randomly dispersed. Consequently, based on the diagnostic examination performed, the residuals satisfy the properties of white noise—being
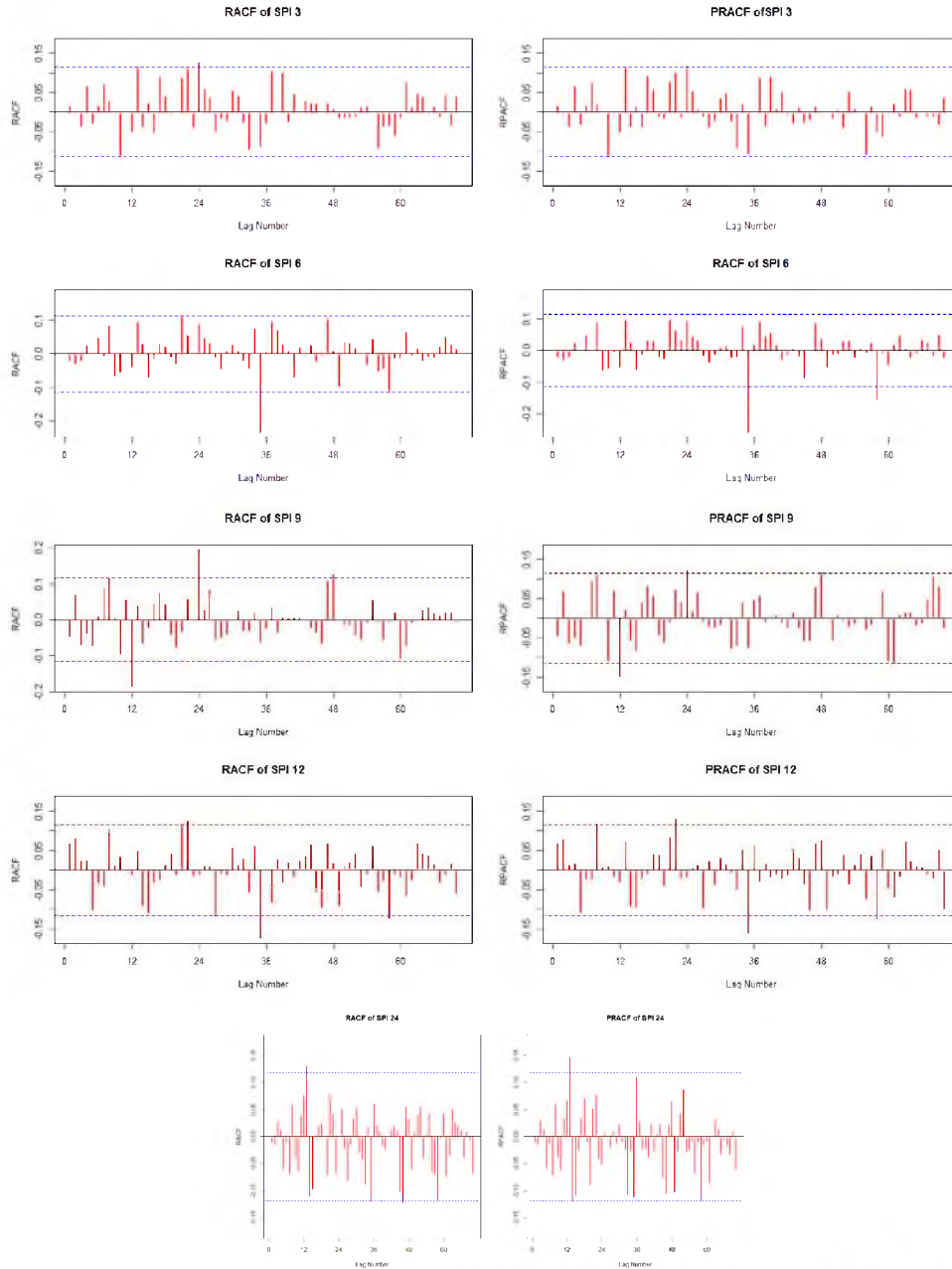
Figure 5. The ACF and PACF of residuals of SPI values in different time scales.

uncorrelated, conforming to a normal distribution, displaying random scattering, and maintaining constant variances. Consequently, we can deduce that the selected models are appropriate for the respective SPI time scales.

4.4   Model Validation

At this stage of analysis, data from 2016 to 2020 were utilized for model validation. Figure 8 represents a comparison of observed values and predicted amounts which it can be easily found that
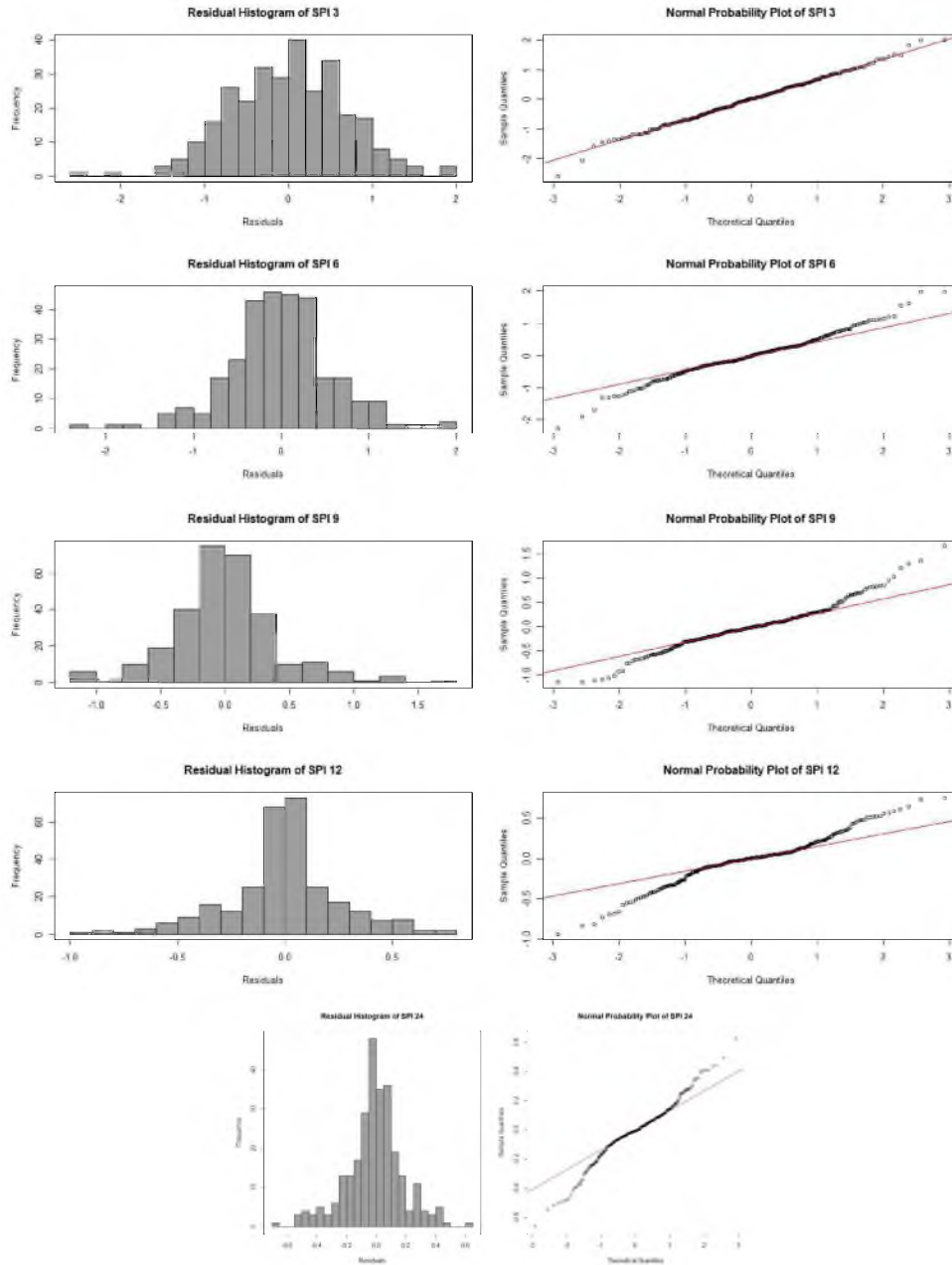
Figure 6. The histogram (left column) and normal probability plot (right column) of residuals at different SPI series.

the predicted values produced a similar pattern to the observed data. The analysis of our forecasting model's performance in Table 5 reveals intriguing insights, particularly when considering the SPI values. As the SPI values increase from 3 to 24, we observe a consistent trend of decreasing RMSE and MAE, indicative of an enhanced absolute forecasting accuracy. This signifies that our model excels in accurately predicting the magnitude of drought events as we extend the forecasting horizon. However, the standout feature of our analysis is the relatively high MAPE exhibited, especially in cases like SPI 3 and SPI 6, where MAPE values exceed 100%. This discrepancy can be attributed
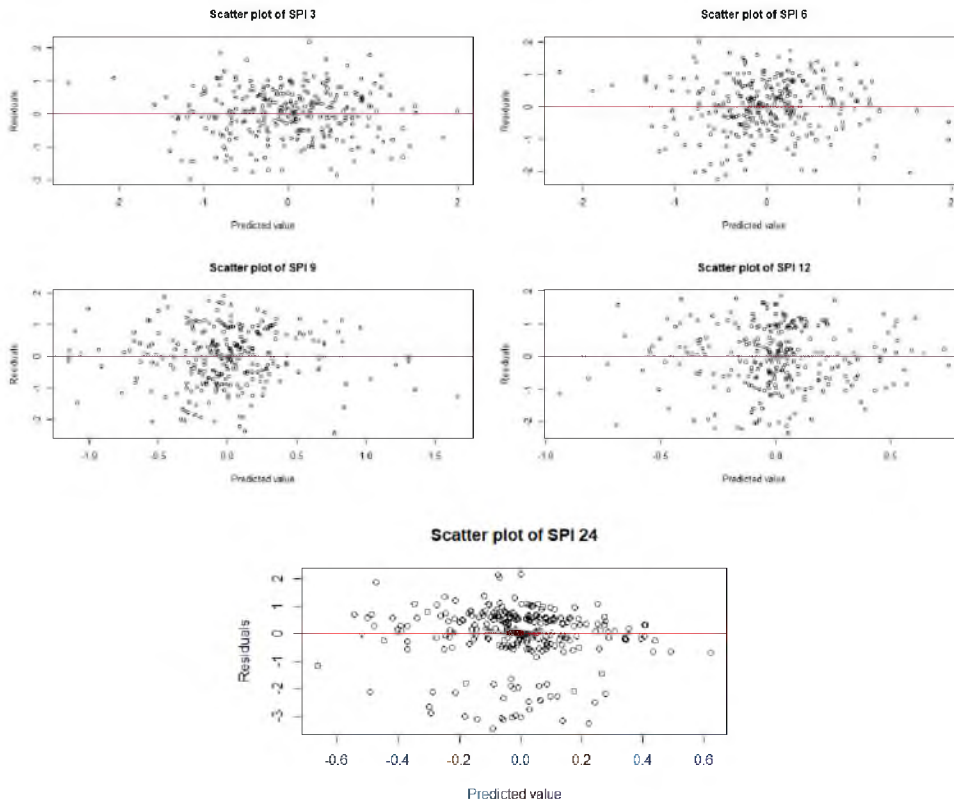
Figure 7. The scatterplot of the residuals against predicted values of each SPI series.

to the unique nature of our data, which hovers close to zero, causing small forecasting errors to result in disproportionately high percentage errors. It's crucial to appreciate that the high MAPE values stem from the inherent scale of our data and its proximity to zero, rather than reflecting a failure in our model's forecasting ability. Instead, they serve as a reminder of the importance of considering the specific context and nature of the data when interpreting forecasting accuracy metrics. Furthermore, the consistently lower RMSE and MAE values at higher SPI values underscore the model's proficiency in absolute forecasting accuracy as the SPI horizon extends.

Please add the following required packages to your document preamble:

4.5   Forecasting

Predicting future drought events holds paramount significance in strategic planning to mitigate the societal and environmental repercussions of drought. In our study, we harnessed state-of-the-art ARIMA and SARIMA models to forecast drought occurrences in Afghanistan for the upcoming year. The results, graphically depicted in Figure 9 with 80 and 95 percent confidence intervals, exhibit a stochastic nature, highlighting the dynamic changes inherent in each SPI time series. In general, our findings indicate that extreme drought conditions are not anticipated for the following year. However, the nation is poised to encounter conditions spanning from near-normal to moderate drought. These results emphasize the seasonal variability in drought occurrences, with a preference for manifestation during the summer and winter months.
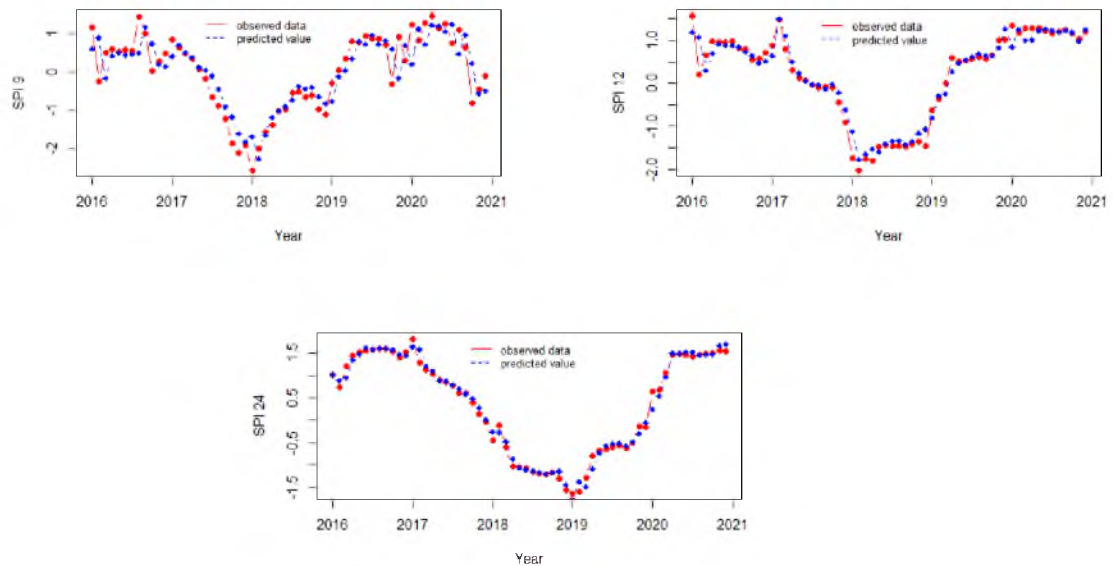
Figure 8. Comparison of observed data with predicted values using the best ARIMA model at each SPI series.

Upon closer examination of the analytical outcomes, it becomes evident that the lowest SPI values are predominantly concentrated in the summer and winter periods, signaling a looming shortage of rainfall and precipitation. Given that a substantial portion of the country's precipitation falls as snow, any deviations from the traditional winter precipitation patterns, coupled with the projected decline in precipitation from July to December, pose adverse implications for Afghanistan's agriculture sector. Reduced precipitation adversely impacts the agricultural landscape by constraining water resources for irrigation, inducing drought-induced stress, obstructing crop growth and maturation, heightening vulnerability to pests and diseases, and compromising livestock grazing and productivity.

5   Conclusion

In this study, stochastic time series modeling was employed to predict drought occurrences in Afghanistan. The monthly average precipitation data from 1991 to 2020 were utilized for this purpose. The model development encompassed three key steps: model identification, parameter estimation, and diagnostic checking. During the initial phase of model identification, the optimal ARIMA/SARIMA models were selected for each SPI time scale, guided by the minimization of AIC and BIC values. The parameter estimation stage unveiled that all of model parameters held significance, rendering them suitable for inclusion in the final models. The diagnostic checking further affirmed that the candidate models adhered to white noise conditions, exhibiting constant variance and uncorrelated residuals. To validate the models, data from 2016 to 2020 were utilized. Model adequacy was evaluated using metrics such as RMSE, MAE, and MAPE. The outcomes indicated the models' adequacy, as evidenced by their low and statistically significant RMSE, MAE values. Subsequently, the ARIMA/SARIMA model was employed to predict one year ahead. The SPI values for winter and
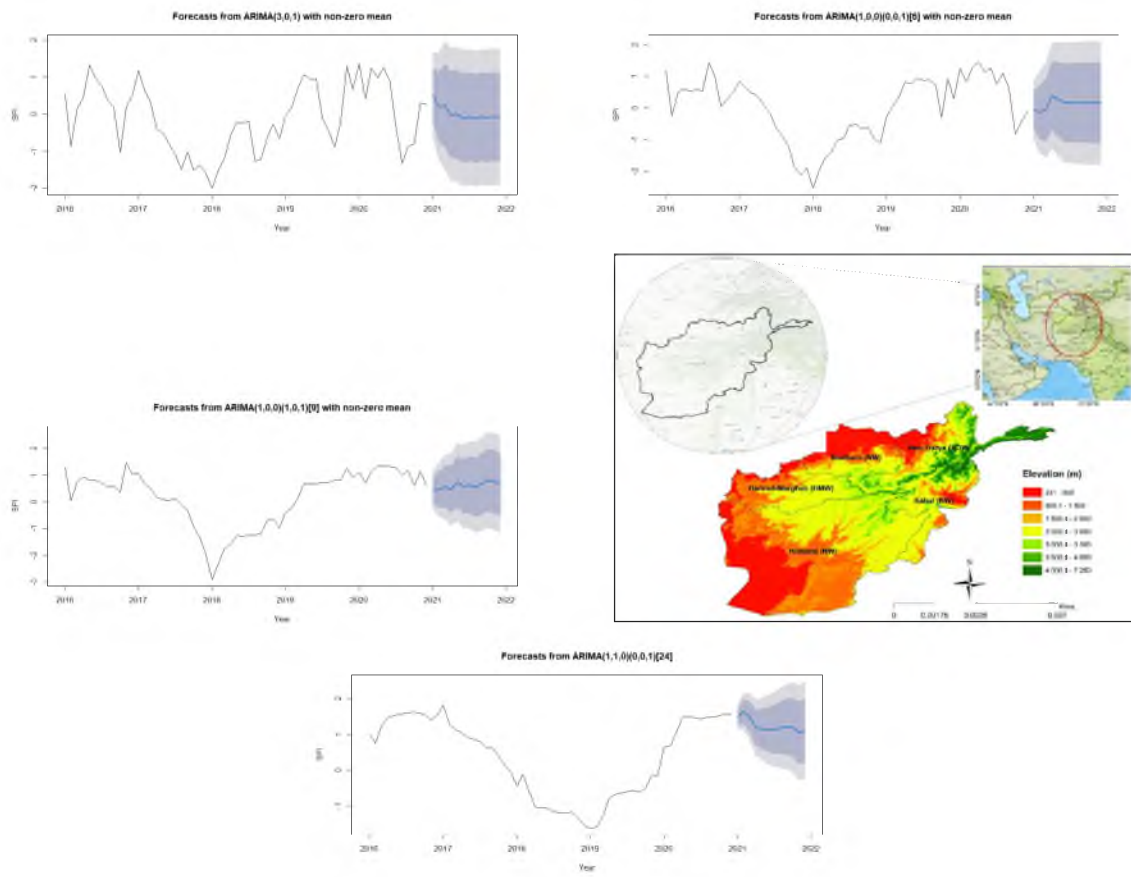
Figure 9. Forecasting drought of one year ahead using the ARIMA/SARIMA model in Afghanistan.

summer indicated a tendency towards near-normal to moderate drought during this period, particularly from July to December.

It is important to note that the study's data comprised monthly average precipitation from across the entire country, thereby offering a generalized overview of Afghanistan's precipitation patterns. Consequently, the results may not be specifically applicable to distinct regions of the country, with some areas potentially experiencing more or less severe drought episodes.

Acknowledgment

References

[1] Mishra, A. K. and Desai, V. R. Drought forecasting using stochastic models. *Stochastic environmental research and risk assessment.* 2005. 19(5): 326–339, doi: 10.1007/s00477-005-0238-4.

[2] Yihdego, Y. Vaheddoost, B. and Al-Weshah R. A. Drought indices and indicators revisited. *Arabian Journal of Geosciences.* 2019: 12(3). doi: 10.1007/s12517-019-4237-z.

[3] Eslamian, S. Ostad-Ali-Akbari, K. Singh Vijay P. and Dalezios Nicolas R. A Review of Drought Indices. *Int. J. Constr. Res. Civ. Eng..* 2017. 3(4) doi: 10.20431/2454-8693.0304005.

[4] Eslamian, S. *Handbook of Engineering Hydrology.* CRC Press, 2014.

[5] Wilhite, D. A. Glantz, M. H. and Glantz, M. H. Understanding the Drought Phenomenon:The Role of Definitions. 1985. [Online]. Available: http://digitalcommons.unl.edu/droughtfacpubhttp://digitalcommons.unl.edu/droughtfacpub/20

[6] Wilhite, D. A. Ed. *Drought and Water Crises.* CRC Press, 2005.

[7] Rafiei-Sardooi, E. Mohseni-Saravi, M. Barkhori, S. Azareh, A. Choubin, B. and Jafari-Shalamzar, M. Drought modeling: a comparative study between time series and neuro-fuzzy approaches. *Arabian Journal of Geosciences.* 2018. 11(17):1-9. doi: 10.1007/s12517-018-3835-5.

[8] Anshuka, A. van Ogtrop, F. F. and Willem Vervoort, R. Drought forecasting through statistical models using standardised precipitation index: a systematic review and meta-regression analysis. *Natural Hazards.* 2019. 97(2): 955-977. doi: 10.1007/s11069-019-03665-6.

[9] Hayes, M. Svoboda, M. Wall ,N. and Wi dhalm,M. The Lincoln Declaration on Drought Indices: Universal Meteorological Drought Index Recommended. *Bulletin of the American Meteorological Society.* 2011. 92(4): 485-488. doi: 10.1175/2010BAMS3103.1.

[10] Guttman, N. B. Comparing the palmer drought index and the standardized precipitation index. *JAWRA Journal of the American Water Resources Association.* 1998. 34(1): 113-121. doi: 10.1111/j.1752-1688.1998.tb05964.x.

[11] Zargar, A. Sadiq, R. Naser, B. and Khan, F. I. A review of drought indices. *Environmental Reviews* .2011. 19(NA): 333-349. doi: 10.1139/a11-013.

[12] Mossad, A. and Alazba, A. Drought Forecasting Using Stochastic Models in a Hyper-Arid Climate. *textAtmosphere*. 2015. 6(4): 410-430. doi: 10.3390/atmos6040410.

[13] Durdu, Ö. F. Application of linear stochastic models for drought forecasting in the Büyük Menderes river basin, western Turkey. *Stochastic Environmental Research and Risk Assessment* . 2010. 24(8): 1145-1162. doi: 10.1007/s00477-010-0366-3.

[14] Li, J. Zhou, S. and Hu, R. Hydrological Drought Class Transition Using SPI and SRI Time Series by Loglinear Regression. *Water resources management*. 2016. 30(2): 669-684. doi: 10.1007/s11269-015-1184-7.

[15] Park, S. Im, J. Jang, E. and Rhee, J. Drought assessment and monitoring through blending of multi-sensor indices using machine learning approaches for different climate regions. *Agricultural and forest meteorology*. 2016. 216: 157-169. doi: 10.1016/j.agrformet.2015.10.011.

[16] Deo, R. C. and Şahin, M. Application of the Artificial Neural Network model for prediction of monthly Standardized Precipitation and Evapotranspiration Index using hydrometeorological parameters and climate indices in eastern Australia. *Atmospheric research* . 2015. 161: 65-81. doi: 10.1016/j.atmosres.2015.03.018.

[17] Belayneh, A. Adamowski, J. and Khalil, B. Short-term SPI drought forecasting in the Awash River Basin in Ethiopia using wavelet transforms and machine learning methods. *Sustainable Water Resources Management*. 2016. 2(1): 87-101. doi: 10.1007/s40899-015-0040-5.

[18] Jalalkamali, A. Moradi, M. and Moradi, N. Application of several artificial intelligence models and ARIMAX model for forecasting drought using the Standardized Precipitation Index. *International journal of environmental science and technology* . 2015. 12(4): 1201-1210. doi: 10.1007/s13762-014-0717-6.

[19] Rahmat, S. N. Jayasuriya, N. and Bhuiyan, M. A. Short-term droughts forecast using Markov chain model in Victoria, Australia. *Theoretical and Applied Climatology*. 2017. 129: 445-457. doi: 10.1007/s00704-016-1785-y.

[20] Dehghani, M. Saghafian, B. Rivaz, F. and Khodadadi, A. Evaluation of dynamic regression and artificial neural networks models for real-time hydrological drought forecasting. *Arabian Journal of Geosciences* . 2017. 10(12): 1-13. doi: 10.1007/s12517-017-2990-4.

[21] Adnan, R. M. Yuan, X. Kisi, O. and Curtef, V.Application of time series models for streamflow forecasting. *Application of time series models for streamflow forecasting.*. 2017. 9(3): 56-63.

[22] Rezaiy, R. and Shabri, A. Drought forecasting using W-ARIMA model with standardized precipitation index. *Journal of Water and Climate Change*. 2023. 14(9): 3345-3367. doi: 10.2166/wcc.2023.431

[23] Alsharif, M. H. Younes, M. K. and Kim, J. Time series ARIMA model for prediction of daily and monthly average global solar radiation: The case study of Seoul, South Korea. *Symmetry*. 2019. 11(2): 240. doi: 10.3390/sym11020240.

[24] Jadin, J. Afghanistan Drought response USD 30 million 10.6 million people severely food insecure. 2018. [Online]. Available: www.fao.org/emergencies.

[25] Assem Mayar, M. Droughts on the Horizon: Can Afghanistan manage this risk? Afghanistan-analysts.org, Feb. 07, 2021.

[26] World Meteorological Organization (WMO) (2011) Proceedings of an Expert Meeting 2–4 June, 2010, Murcia, Spain.

[27] Thomas, B. McKee, N, Doesken, J. and Kleist, J. Analysis of Standardized Precipitation Index (SPI) data for drought assessment. *Water (Switzerland)*. 1993. 26(2). doi: 10.1088/1755-1315/5.

[28] Thom, H.C. A note on the gamma distribution. *Monthly weather review*.1958.86(4):117-122

[29] Guttman, N.B. Accepting the standardized precipitation index: a calculation algorithm 1. *JAWRA Journal of the American Water Resources Association*, 1999, 35(2):311-322. doi: 10.1111/j.1752-1688.1999.tb03592.x.

[30] Box, G. E. and Jenkins, G. *Time series Analysis: Forecasting and Control*. San Francisco: Holden-Day, 1976.

[31] Box, E. P. Jenkins, G. M. and Reinsel, G. C. *Time Series Analysis: Forecasting and Control*, 3rd ed. New Jersey: Prentice Hall, 1994.

[32] Modarres, R. Streamflow drought time series forecasting. *Stochastic Environmental Research and Risk Assessment*. 2007. 21(3): 223-233. doi: 10.1007/s00477-006-0058-1.

[33] Box, E. P. Jenkins, G. M. and Reinsel, G. C. *Time Series Analysis: Forecasting and Control*, 3rd ed. New Jersey: Prentice Hall, 1994.

[34] Brockwell, P.J. and Davis, R.A. *Introduction to Time Series and Forecasting*. Springer Science and Business Media LLC Berlin/Heidelberg, Germany, 2016.

[35] Akaike, H. A New look at the statistical model identification. *IEEE Transactions on Automatic Control*. 1974. 19(6): 716-723. doi: 10.1109/TAC.1974.1100705.

[36] Schwarz, G. Estimating the dimension of a model. *Ann. Stat*. 1978. 6(2): 461–464.

[37] Kulahci, M. Montgomery, D. C. and Jennings, C. L. *Introduction to Time Series Analysis and Forecasting*. 2nd ed. United Kingdom: Wiley, 2015.

[38] Mahmud, I. Bari, S. H. and Rahman, M. T. U. Monthly rainfall forecast of Bangladesh using autoregressive integrated moving average method. *Environmental Engineering Research*. 2016. 22(2): 162-168. doi: 10.4491/eer.2016.075.

[39] Yeh, H. F. and Hsu, H. L. Stochastic model for drought forecasting in the Southern Taiwan basin. *Water*. 2019. 11(10): 2041. doi: 10.3390/w11102041.

[40] Rahman, M. A. Yunsheng, L. and Sultana, N. Analysis and prediction of rainfall trends over Bangladesh using Mann–Kendall, Spearman's rho tests and ARIMA model. *Meteorology and Atmospheric Physics*. 2017. 129(4): 409-424. doi: 10.1007/s00703-016-0479-4.

[41] Putro, S. P., Koshio, S., and Oktaferdian, V. Implementation of ARIMA Model to Asses Seasonal Variability Macrobenthic Assemblages. *Aquatic Procedia*. 2016. 7: 277-284. doi: 10.1016/j.aqpro.2016.07.039.